

Improved Interactive Visualization of Magnetic Flux Lines in 3-D Space Using Edge Finite Elements

Vlatko Cingoshi, Tsuyoshi Kuribayashi, Kazufumi Kaneda and Hideo Yamashita
Faculty of Engineering, Hiroshima University, Kagamiyama 1-4-1 Higashi-hiroshima, 739 JAPAN

Reprinted from
IEEE TRANSACTIONS ON MAGNETICS
Vol. 32, No. 3, May 1996

Improved Interactive Visualization of Magnetic Flux Lines in 3-D Space Using Edge Finite Elements

Vlatko Čingoski, Tsuyoshi Kuribayashi, Kazufumi Kaneda and Hideo Yamashita
Faculty of Engineering, Hiroshima University, Kagamiyama 1-4-1 Higashi-hiroshima, 739 JAPAN

Abstract—In this paper, improved method for interactive visualization of magnetic flux lines in 3-D space is presented. The problem of determining the number of flux lines and their starting position is treated and solved using a simple and computationally efficient algorithm which incorporates the intensity values of magnetic flux density and several appropriate weighted functions. The solenoidal characteristic of magnetic flux density distribution, which results in magnetic flux lines becoming closed lines, is also successfully treated by means of edge finite elements. The procedure and examples to demonstrate the advantages of the proposed method are also presented.

I. INTRODUCTION

Recent developments in computational technology have enabled the analysis of increasingly complex and higher-dimensional problems with ease even on small or personal computers. At the same time, post-processing techniques also have undergone tremendous development, especially in the domain of scientific visualization, simulation and animation. The main goal of these developments is to assist in the estimation and evaluation of computational results and in understanding their physical meaning. Displaying the intensity distribution of a vectorial quantity, such as magnetic vector potential or flux density, is not sufficient because it only allows visualization of the intensity values, not their direction and loci. For an easy understanding of the physical behavior of the magnetic field phenomena, therefore, visualization of the magnetic flux lines is somehow necessary. Using magnetic flux lines, the analyst can clearly understand not only the physical meaning of the analyzed magnetic field, but also its direction, magnitude and loci. If this visualization process is interactive, the analyst becomes an active subject in the analysis process which is especially beneficial for designing various electromagnetic devices.

The authors have already presented several papers on the phenomenon of the visualization of magnetic fields [1], [2], [3]. Some problems regarding the visualization of magnetic flux lines remain, however, especially in 3-D space:

- Definition of the number of lines and position of the starting point from which each magnetic flux line emerges.
- Satisfaction of the solenoidal characteristic of magnetic flux lines – the flux lines must be closed and smooth enough to correctly represent the physical behavior of the magnetic field.
- Extension of the interactivity level, a very important factor for a more sophisticated approach in magnetic field analysis, especially for end-users with little experience.

In this paper, the authors propose an improved interactive visualization method, one which efficiently deals with each of the above-mentioned problems. For solving the first problem, a relatively simple procedure is proposed for determining the nearly optimal position of each magnetic flux line's starting point, which lies in the high-field area. The procedure employs the magnetic flux density values and appropriate weighted functions. The second problem is solved using edge finite elements that provide a normal continuity of magnetic flux density vector \mathbf{B} across any inter-material boundaries. The procedure and some useful examples that convey the advantages of the proposed method are presented.

II. PROPOSED METHOD

As previously mentioned, in this paper we propose an algorithm for interactive visualization of magnetic flux lines in 3-D space applied over an edge finite element division mesh that successfully overcomes the above mentioned problems. Next, we briefly discuss the main points of the proposed algorithm.

A. Determination of number and starting point of magnetic flux lines

Observing the magnetic flux lines allows the observer to obtain information regarding the vectorial field's direction and loci. In order to easily understand the behavior of the field, a magnetic flux line distribution with a large number of lines in the high-field area and a small number of lines in the low-field area is desired.

Manuscript received July 10, 1995.

To realize this, the starting positions of magnetic flux lines should be defined first. If the positions are defined randomly in 3-D space with high and low-field areas, some flux lines will occasionally overlap each other. To avoid this problem, instead of definition of the starting points of magnetic flux lines, in this paper we propose definition of a common plane S from which the flux lines will emerge. The proposed algorithm is as follows:

- Define the value of the total number of flux lines N_{total} , and a plane S in 3-D space from which all flux lines will emerge by the user.
- Divide plane S into sub-planes using a lattice division, which will aid in the easy computation of the number of lines and their starting position (Fig. 1a). Next, magnetic flux densities B_j at grid points are obtained from the results of finite element analysis.
- Define the average flux value for each sub-plane i using the following equation

$$\bar{\Phi}_i^{Average} = \frac{\sum_{j=1}^4 B_j}{4} \cdot S_i, \quad (1)$$

where i is the number of the sub-plane, B_j is the intensity of magnetic flux density at the four corner points, and S_i is the area of sub-plane i (see Fig. 1).

- Compute the number of flux lines in each sub-plane i using the following equation

$$N_i = \frac{\bar{\Phi}_i^{Average}}{\sum_{k=1}^n \bar{\Phi}_k^{Average}} \cdot N_{total}, \quad (2)$$

where n is the total number of sub-planes, N_{total} is the total number of flux lines and $\bar{\Phi}_k^{Average}$ is the average flux value for each respective sub-plane. An example of the above described procedure is presented in Fig. 2. Figure 2a shows the number of flux lines N_i per each sub-plane S_i .

- Randomly determine the temporary starting point (x_{temp}, y_{temp}) of each flux line in each sub-plane. These points are marked with "x" in Fig. 2b.

However, the positions of temporary starting points are independent of the intensity of magnetic flux density in each sub-plane. In order to take into account the intensity of magnetic flux density in each sub-plane, each temporary starting point is moved to an area where there is a high concentration of magnetic flux density. The following procedure determines the final starting point (x_{final}, y_{final}).

- For each sub-plane, find the center of gravity (see Fig. 2b) and the central point of magnetic flux density

with coordinates defined by the following equations (see Figs. 1b and 2c):

$$x = \frac{B_2 + B_3}{\sum_{j=1}^4 B_j} \cdot \Delta x, \quad y = \frac{B_3 + B_4}{\sum_{k=1}^4 B_j} \cdot \Delta y. \quad (3)$$

- By correspondence between the center of gravity in Fig. 2b and the central point of magnetic flux density in Fig. 2c, four rectangles of each sub-plane in Fig. 2b are mapped to new four rectangles as shown in Fig. 2c.
- The temporary starting point is then mapped to its appropriate position using conform mapping between the initial rectangular area of the sub-plane and its new distorted rectangular area, resulting in the final position of the starting point for each flux line, as shown in Fig. 2c.

In this way, we can get a large number of magnetic flux lines emerging from the high-field area. Next, we describe a method for calculating the magnetic flux lines that satisfies the solenoidal characteristic.

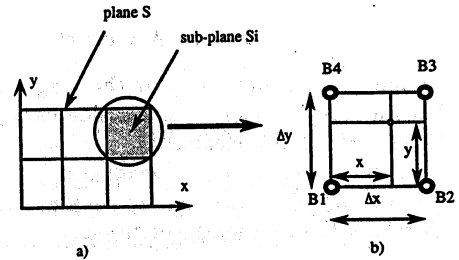


Fig. 1. Plane S with its sub-planes.

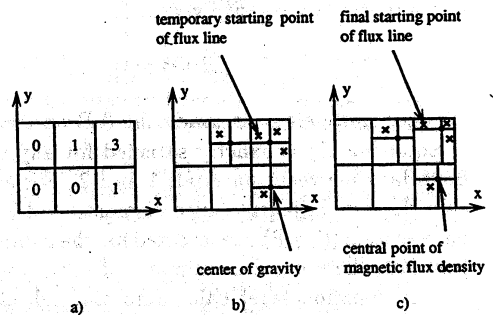


Fig. 2. Definition of number of lines.

B. Solenoidal characteristic of magnetic flux lines

As previously mentioned, in this paper the problem of satisfying the solenoidal characteristic of the magnetic flux lines, and the magnetic field in general, is solved using edge finite elements. In Fig. 3a, a typical first-order edge-based finite element is presented. It has six edges and six unknown scalar values of the circulation of magnetic vector potential A along each of its edges A_i . Approximation of the potential inside the finite elements is made possible by the vectorial shape functions N_i , ($i = 1, 2, \dots, 6$), by the following equation.

$$\mathbf{A} = \sum_{i=1}^6 N_i A_i \quad (4)$$

Here, magnetic vector potential \mathbf{A} obtained by edge finite element analysis has the following characteristic:

$$\mathbf{A} = \begin{Bmatrix} A_x \\ A_y \\ A_z \end{Bmatrix} = \begin{Bmatrix} f(y, z) \\ f(x, z) \\ f(x, y) \end{Bmatrix}. \quad (5)$$

That is, the x component of the magnetic vector potential A_x is a function of only y and z coordinates. Magnetic flux density \mathbf{B} is calculated using the magnetic vector potential \mathbf{A} computed using (5), that is, \mathbf{B} is given by (6).

$$\mathbf{B} = \text{rot} \mathbf{A} = \text{const.} \quad (6)$$

From (6) it is obvious that the magnetic flux density \mathbf{B} maintains a constant value inside each finite element, as first-order finite elements are employed. In addition, the normal components of magnetic flux density vector \mathbf{B} across any element facet are constant and continuous. Therefore, the continuity condition

$$\mathbf{n} \cdot (\mathbf{B}_1 - \mathbf{B}_2) = 0. \quad (7)$$

is satisfied across any facet between two adjacent finite elements without any constraint [4]. This condition leads to the perfect satisfaction of the solenoidal characteristic of magnetic flux density vector \mathbf{B}

$$\text{div} \mathbf{B} = 0 \quad (8)$$

for each finite element inside the 3-D analysis region.

Equation (7) is exactly satisfied for any inter-material boundary between materials 1 and 2. For example, if we consider two adjacent finite elements and a local coordinate system (ζ, η, ξ) constructed for the common facet (see Fig. 3b), the normal component of magnetic flux density on the common facet calculated through element 1 and element 2 separately could be

$$B_{\zeta_1} = \left(\frac{\partial A_{\eta}}{\partial \xi} - \frac{\partial A_{\xi}}{\partial \eta} \right)_1 = \left(\frac{\partial A_{\eta}}{\partial \xi} - \frac{\partial A_{\xi}}{\partial \eta} \right)_2 = B_{\zeta_2}. \quad (9)$$

It is obvious that the normal component of magnetic flux density depends only on tangential components of magnetic vector potential \mathbf{A} that are the same for both adjacent finite elements. The normal continuity of magnetic flux density, therefore, is ensured between any two adjacent finite elements which in turn ensures the satisfaction of the solenoidal characteristic of the magnetic flux lines and of the field itself.

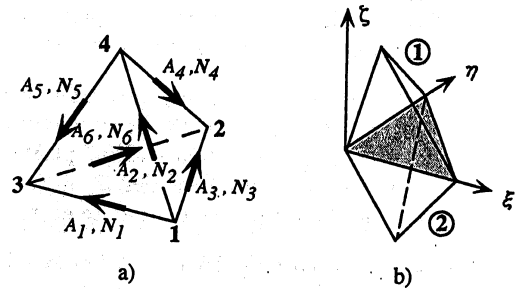


Fig. 3. Edge finite elements.

C. Interactivity

Using powerful graphics workstations (SGI Indigo²), we developed a sophisticated visualization method for fully interactive processing of the magnetic flux lines.

The visualization method performs functions like definition of the plane from which the flux lines emerge and of the desired number of flux lines, and also the development of a user-friendly menu for manipulation of the obtained flux line distribution in 3-D display space. The developed interactive menu is illustrated, in Fig. 4

The procedure for interactive visualization of magnetic flux line is as follows:

Step 1 Definition of desired number of flux lines:

Click the mouse button inside area $\langle a \rangle$, and input the desired number of flux lines from the keyboard.

Step 2 Definition of the plane from which the flux lines emerge:

By clicking one of the buttons $\langle b \rangle$, choose one plane within the xy, yz, zx planes. The z, x, y coordinates are determined using slidebar $\langle c \rangle$.

Step 3 Determination of starting points of flux lines:

By clicking button $\langle d \rangle$, the starting points of flux line are calculated using the method described in section II.A. Starting points are displayed in display area $\langle e \rangle$.

Step 4 Calculation and display of flux lines:

By clicking button $\langle f \rangle$, calculation of flux lines is executed using the method described in section II.B, and the magnetic flux lines are displayed.

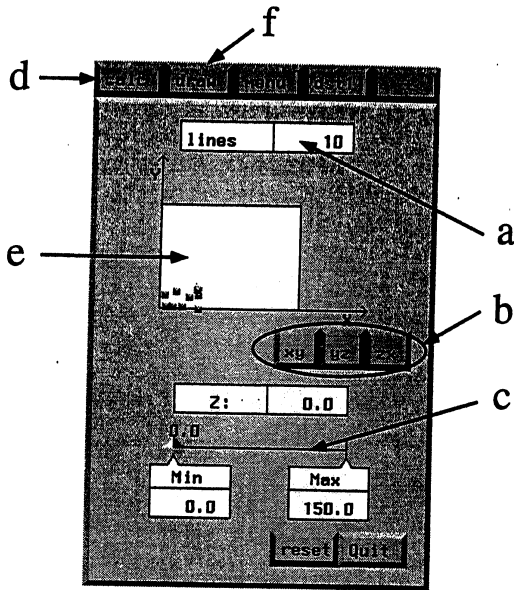


Fig. 4. Interactive menu.

The user easily gets an effective display of the 3-D vector field by using steps 1, ..., 4. Steps 1 and 2 are part of the user's input, and steps 3 and 4 are part of the calculation. Steps 3 and 4 only take about one second to calculate and display about ten magnetic flux lines simultaneously, which is about twenty times faster than our previous method [3]. After displaying the magnetic flux lines, the user can interactively observe and examine the obtained 3-D flux line distribution using a free rotation and zoom technique.

III. APPLICATIONS

In order to verify the usefulness of the proposed method, a test model is used. The model consists of a rectangular core surrounded by a rectangular coil and two aluminum plates. Each plate has a hole, and the plates are symmetrically set above and below the core.

With the proposed method, the distribution of magnetic flux lines using plane $z = 0$ as a plane S from which flux lines emerge is computed and presented in Figs. 5. From Figs. 5a and b, it is readily apparent that a large number of flux lines emerge from the core area where magnetic flux density is high. Some flux lines are obstructed by the aluminum plate, while others can freely penetrate inside the hole of the aluminum plate.

IV. CONCLUSION

An improved method for interactive visualization of magnetic flux lines in 3-D space was presented. The prob-

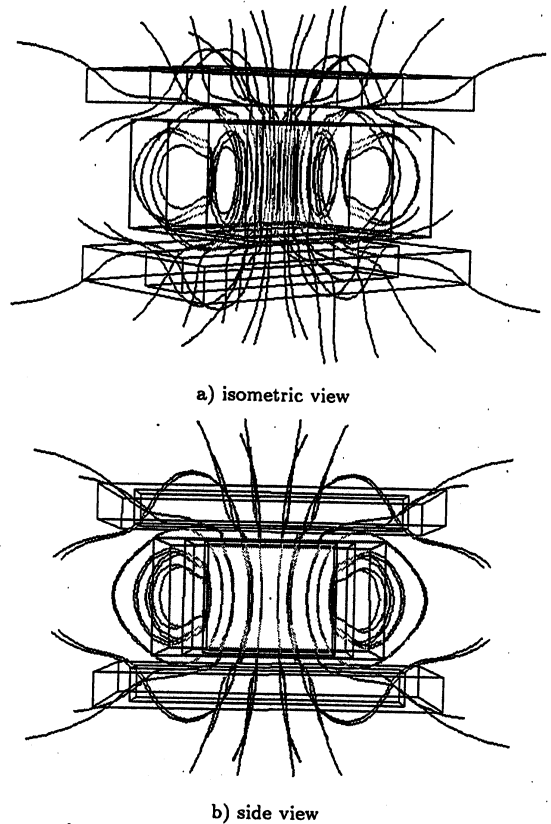


Fig. 5. Obtained distribution of magnetic flux lines.

lem of determining the number of flux lines and their starting position was solved by using a simple and computationally efficient algorithm which incorporates the intensity values of magnetic flux density and several appropriate weighted functions. The solenoidal characteristic of magnetic flux density distribution was also successfully solved by means of edge finite elements.

REFERENCES

- [1] H. Yamashita, K. Harada, E. Nakamae, J. Itano, and M. S. A. A. Hamman, "Stereo graphic display on three dimensional magnetic fields of electromagnetic machines," *IEEE Trans. Power Apparatus and Systems, PAS-100*, No. 6, 1981, pp. 4692-4697.
- [2] H. Yamashita, T. Johkoh, S. Takita, and E. Nakamae, "Interactive visualization of three-dimensional magnetic fields," *The Journal of Visualization and Computer Animation*, vol. 2, 1991, pp. 34-40.
- [3] V. Čingoski, M. Ichinose, K. Kaneda, and H. Yamashita, "Analytical calculation of magnetic flux lines in 3-D space," *IEEE Transaction on Magnetics*, vol. 30, No. 5, September 1994, pp. 2912-2915.
- [4] M. L. Barton and Z. J. Cendes, "New vector finite elements for three-dimensional magnetic field computation," *Journal of Appl. Phys.*, vol. 61, No. 8, 15 April 1987, pp. 3919-3921.